Circular Hall Transducer for Accurate Contactless Angular Position Sensing

Laurent Sache*, Serge Reymond**, Pavel Kejik**, Mikael Sjöholm*, Daniel Bommottet*, Volker Gass*, Lionel Gaillard+ and Radjan S. Popovic**

Abstract

Demands for robust, reliable and accurate angular position sensing of space mechanism are increasing steadily. As a consequence, contactless sensors providing an alternative to triblogical drawbacks of the current sliding potentiometers represent a key factor for the development of future space applications. In the framework of the ESTEC activity [1] covering the selection of an angular position sensor (APS) based on MEMS technology and in collaboration with the EPFL-LMIS [2], RUAG is currently carrying out the qualification of a new contactless angular position sensor based on the Hall Effect. Providing the angle without need of a complex algorithm, it offers a more reliable, lighter, less sensitive to vibrations and cost effective sensing solution.

Introduction

Current rotary sensors are either potentiometers or encoders. Be it in the case where those systems are placed on the outside or on the inside of the satellite bus, the environmental conditions are typically very harsh.

Potentiometers cover low accuracy application in a range down to 0.4°. They have the advantage of simplicity, size, ease of implementation and low cost. Rotor and stator (track) typically have to be installed independently but this process is not extremely sensitive with regards to the relative alignment of brushes to track. The electrical interface is typically a 0 - 5V analogue one. On the other hand potentiometer reliability suffers from the sliding contact of a metallic brush on a plastic film with implemented conductive materials (carbon, etc). Various combinations of materials with and without lubrication have been applied but sufficient reliability could not be proven so far specifically for long time application like telecom (12 to 15 years). An alternative to such simple device would be the most demanding application.

Encoders are typically used when high resolution and reliability is required but suffer from their complexity of the mechanical integration and the electrical interface. Encoders have a higher mass and in case of high exposure to radiation they have to be additionally shielded by a metallic housing that adds weight. The electrical interface is digital (serial or parallel) and thus more complex to handle compared to the one of a potentiometer. Additionally encoders are expensive and normally come along with long lead times.

The ideal replacement of a potentiometer and/or encoder would be a sensor that combines both positive characteristics:
From the potentiometer:
- simple electrical interface
- simple mechanical interface (low sensitivity to misalignment)
- radiation resistance
- small and low weight
- low cost

From the encoder:
- high resolution

* RUAG Aerospace, Nyon, Switzerland

** Ecole Polytechnique Fédérale de Lausanne (EPFL), Lausanne, Switzerland

+ European Space Research and Technology Centre (ESTEC), Noordwijk, The Netherlands

The proposed angular position sensor is a magnetostatic encoder based on the Hall Effect. Commercial contactless angular sensors are composed of a two-axis sensitive Hall structure combined with rotating permanent magnets [3]. Most of these technologies provide a two-component analog output, which requires a digital signal processor to calculate the angular position of the permanent magnet (traditionally by the use of CORDIC algorithms [4]). The use of a Digital Signal Processor (DSP) increases the complexity of the surrounding electronics and limits the reliability of the sensor in harsh environment conditions. In this context, the new contactless magnetic sensor proposed here [5], based on a circular sensitive structure, provides the angle without need of a complex algorithm.

The full sensor consists of a passive magnets configuration providing a magnetic field and a sensing element located in the plane of the field. This second element is composed of an encapsulated monolithic silicon chip that detects the direction of the magnetic field. The sensing element being aligned with the magnetic rotation axis, this sensor is dedicated to plain shaft application where the magnetic element can be fixed on the rotating shaft and the sensing element can be held by the housing of the structure. A simple sketch of the working principle is presented thereafter:

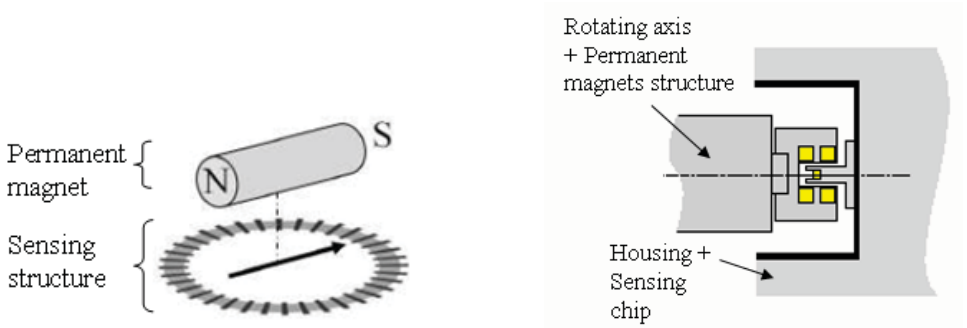

Figure 1. Schematic of the sensor principle (left) and sensor design (right)

This paper describes the sensor and presents the space qualification campaigns that are foreseen in the beginning of 2008.

The first section presents the sensing principle and its associated structure. The subsequent electronic includes in the chip to perform the basic measurement sequence along with the output information treatment is also outlined. A second chapter introduces the magnetic configuration offering the best combination between field homogeneity and sensor accuracy.

The development and the qualification of the sensor arise at two levels and in two steps:

- A first test campaign occurs at the sensor level and is presented in the third chapter. At this level, the electronic layout of the chip is not fully compliant with space standards, as no protection are implemented within the electronic layout with regards to radiation. This first level is a technology level and its main objective is to qualify through a test campaign the whole sensor composed of the rotating element and the sensing element inserted within a Chip On Board (CoB) package. This activity is performed within the framework of an ESA Technology Research Program (TRP) activity [1].

- A second test campaign occurs at chip level and is presented in the fourth section. At this level, the chip is encapsulated within a CERamic Dual In-line Package (CERDIP) and its layout incorporates radiation hardening techniques issue from the radiation test of the first test campaign. Those tests are undertaken at wafer and chip level according to European standards defined for monolithic chip space qualification.

Sensing structure

The sensor consists of a sensing structure, on-chip biasing, signal conditioning circuits and readout interface. The sensing element is an n-doped ring with N contacts equally distributed on the ring surface. Through switches each contact can be connected to the current source, to the ground or to the voltage amplifier. Many different connection combinations give information about the magnetic field. Here we present first a simple measurement sequence, with its associated sensitivity and zero-field offset, and a second sequence with a more efficient offset cancelling.

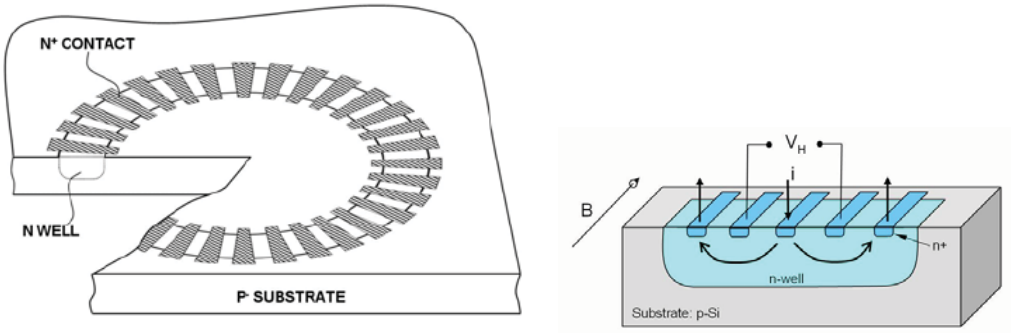

Figure 2. Integrated Hall structure and detail of a 5 Contacts Vertical Hall (5CVH) element

Sensing principle and basic measurement sequence

The measurement sequence is based on a 5 **C**ontacts **V**ertical **H**all element (5CVH) [6] that are composed by 5 in-line contacts. The current is injected through the outer contacts and collected in the middle one. The potential difference between the two remaining contacts (The Hall Voltage V_H) is proportional to one component of the in-plane magnetic field:

$$V_H \ \alpha \ B\cos(\alpha) \qquad (1)$$

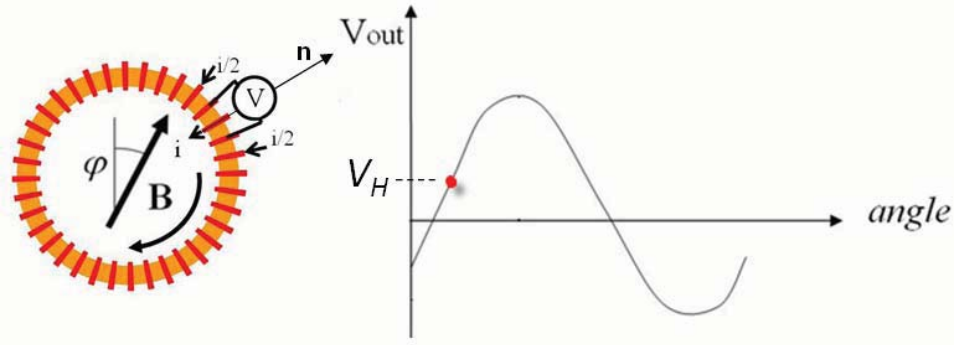

Figure 3. One step of the acquisition of the Hall voltage of one 5CVH.

At a time t, a series of 5 neighbor contacts are connected in such way to form a 5CVH. On a perfect device, the output voltage is proportional to $B\cos(\alpha)$, where α is the angle between **n** (a unitary vector normal to the middle contacts of the 5CVH) and **B**. At each clock time, the 5CVH element is shifted by one contact, and the Hall voltage becomes $B\cos(\alpha+2\pi/n)$. Over a full turn, the Hall voltage exhibits a sine function, with its amplitude proportional to the in-plane field and its phase equal to the field direction. The information about the field direction is contained in the first harmonic over the full turn period.

In a real structure, because of the imperfections (in the material and in the manufacturing process), the Hall voltage is superposed to an offset voltage. The key point is that the one-by-one shift of the 5CVH allows to compensate this offset. This can be easily understood by modeling the Hall ring by a circular array of non-identical resistors (see Figure 4). We can see that the contribution of the i^{th} resistor is cancelled. If a static defect induces an excess of voltage at the output at time *t*, the same defect causes an opposite voltage at time *t+1*. In this ohmic model, the dc offset, i.e. the sum over one full turn is zero.

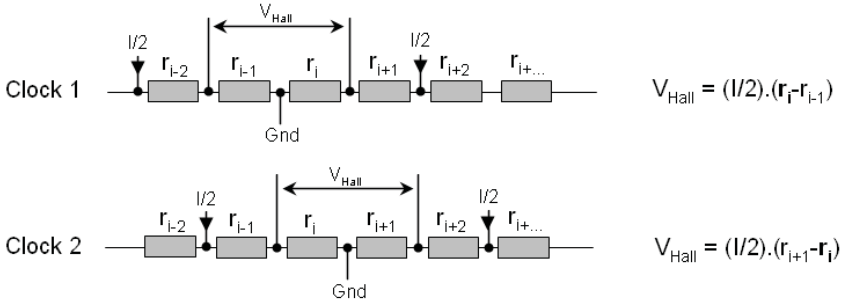

Figure 4. Resistor array model.

Zero field offset

The previous basic measurement sequence does not fully suppress the zero field offset. Even if the dc offset vanishes, a circular array of resistors, randomly distributed, create a non-zero first harmonic. In real devices, additional non-linear effects contribute to increase the offset. The most important one is the junction field effect, which, by squeezing the channel according to the applied voltage causes a dynamic modification of the conductive channel. Combined with the static imperfections, it prevents the full resistance cancellation. As a result, the sum of voltages over one cycle is not zero and degrades the accuracy of the sensor.

Another measurement sequence for suppression of the zero field offset

Depending on the application, another sequence can be implemented for cancelling the offset. A proposed special sequence called “subspinning” can cancels the output voltage; sum over a period much shorter that the full cycle. The aim is to suppress the residual first harmonic of the randomly distributed defects. A particular subspinning sequence is given thereafter on Figure 5.

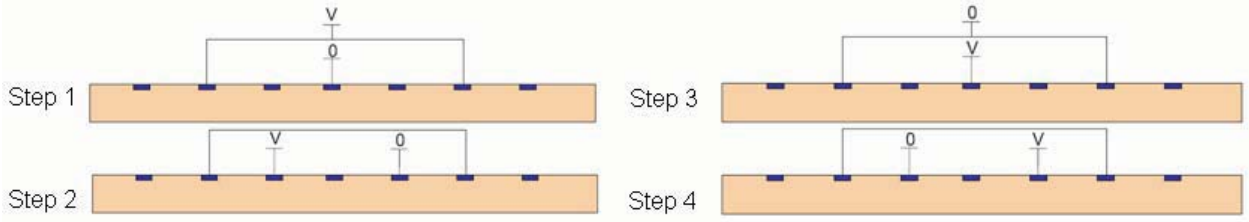

Figure 5. Subspinning sequence for the suppression of the zero offset.

The basic element is also a 5CVH, but the two extreme contacts are shorted and connected to a single current source, in order to make a four terminals device. At each position of the 5CVH, the four connections are circularly permuted, as for usual spinning current method. For a perfect array of resistors the sum over these 4 steps vanishes. As a consequence, the first harmonic is strongly reduced and the offset suppression factor is strongly reduced. Numerical simulations show that the subspinning sequence also suppresses the offset due to junction field effect.

Signal processing and Implementation

The selected technology for the sensor realization is a conventional CMOS 0.35-µm high-voltage technology. The supply voltage is 3.3 V. The sensing part is composed of an n-well ring with 64 n-doped contacts. The ring is formed by a deep n-well layer with about 6 µm of depth. The ring outer diameter is 50 µm. The ring width, contact number, size and shape were determined by optimizing the sensitivity using finite element calculations. A logic circuit ensures the correct switching sequence. The four-phase

subspinning sequence presented above is implemented for the readout of the 5C segments, resulting in 256 (4 x 64) measurement steps per full measurement sequence.

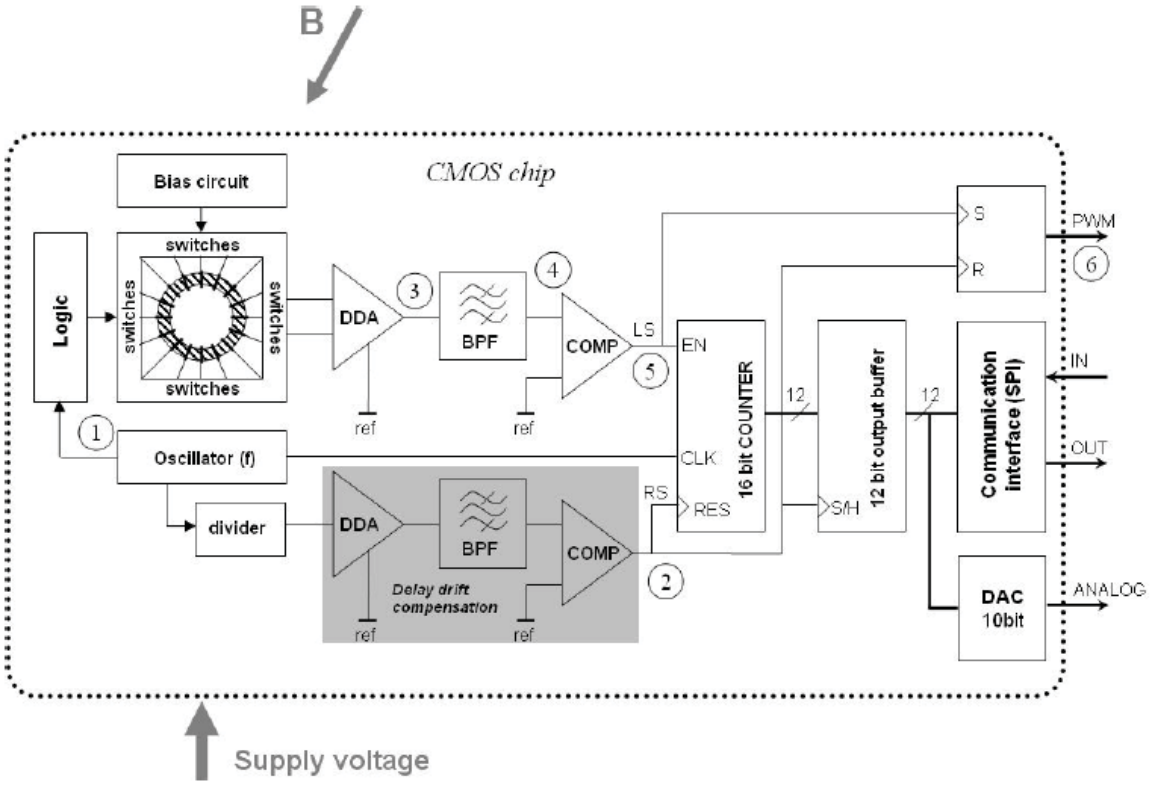

Figure 6. Block diagram of the APS

The measuring principle is based on the phase measurement between the detected signal **(5)** and the reference signal **(2)**. Switches realized by NMOS transmission gates connect the sensing structure to the bias circuit or Differential Difference Amplifier (DDA). The bias current generated in the bias circuit is derived from a bandgap cell. Oscillator, Logic and Divider blocks are realized by digital standard cells available from the foundry. The DDA, Band-Pass Filter (BPF) and Comparator (COMP) are optimized for low-noise, wide temperature range. The output signal is available in three different forms: Pulse Width Modulation (PWM), Serial Peripheral Interface (SPI) and analog output with 10 bits of resolution. Figure 7 shows the main signal waveforms in block diagram. The waveforms are cross-referenced by numbering.

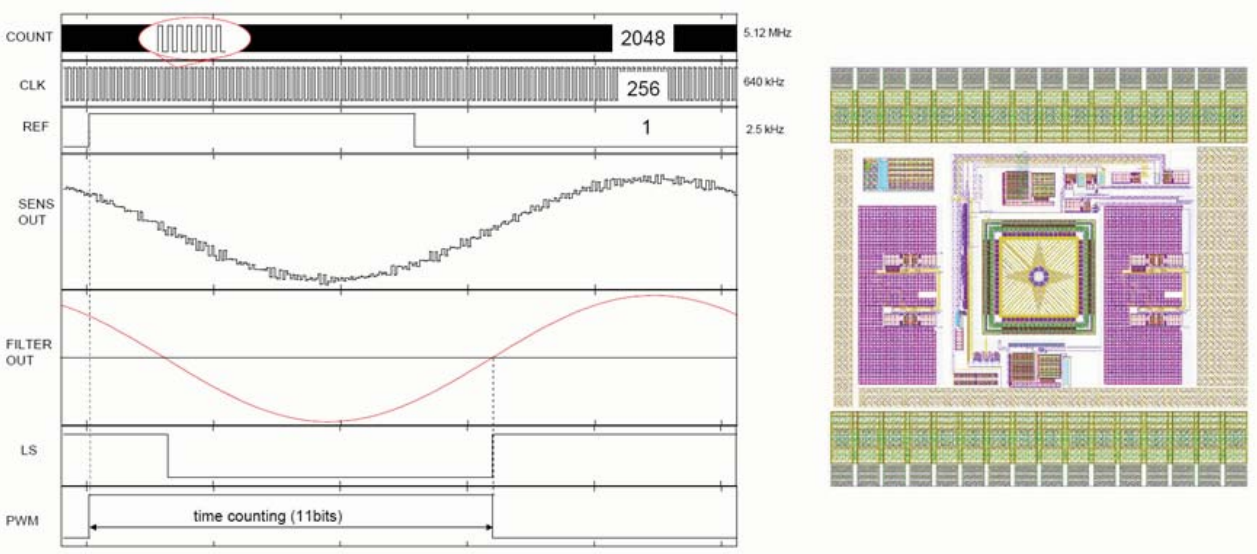

Figure 7. Main signal waveforms (frequency of the clock and reference signal are given for information) and view of the silicon layout.

The Hall voltage coming from the structure **(3)** is sensed and amplified by a differential difference amplifier (DDA) and buffered. The amplification gain is fixed so, that the amplified signal swing is about half of the full supply voltage range (3.3 V). The signal is further filtered through a 4th order band-pass switched capacitor (SC) filter, in order to suppress any high frequency parasitic signals induced by the Hall elements and offsets and 1/f noise caused by the DDA. The choice of the SC filter is due to its excellent stability of the filtering frequency and input-to-output phase shift over temperature. The signal is further filtered through a passive RC low-pass filter with cutoff frequency much higher (at least 10 x cycle frequency) in order to filter the ripple form of the signal coming from the SC filter. The filtered 1st harmonic useful signal (waveform **(4)** in Figure 7) is further transformed into a square wave signal through a comparator (waveform **(5)** in Figure 7). Thereby, the phase of the measured square wave signal can be compared with the reference signal in a logic phase detector circuit COMP **(6)**. In this way, the analog signal is converted to PWM digital form. Such a signal can be further easily converted to a digital word using a counter. Digitalized signal is read via an SPI interface, or converted to the analog form through a DAC. In order to minimize the influence of the phase drift in temperature caused by the electronics on the measured phase, the reference signal is treated in the same way as the detected signal. In other words, the reference signal with adequate magnitude and signal level is fed through a duplicated analog path composed of DDA, SC filter and COMP. In this way both signals are exposed to the same delay drift and the differential drift is minimized.

The sensor conditioning circuit is realized with a bandgap circuit in order to be insensitive to the supply voltage variations and well control the temperature drift of the bias current for the sensing part (Hall element). Since the sensing part is biased with relatively low current to keep the nonlinearity effect low, the drop voltage over the sensing part does not overreach the working range of an N type MOS transistor. Therefore, the sensing part is connected to the conditioning circuit and signal processing circuit via transmission gates composed only by NMOS transistor with optimized size. This allows minimizing the charge injection feed through from a digital driving part to the signal processing path. Chip size is of about 1.9 x 1.9 mm2. The system has 32 bonding pads with a pitch of 120 µm. The sensing part is centered with respect to the chip outlines (see Figure 7). Supply pads of the digital and analog part are split into two parts; in order to isolate the analog part from the digital part and prevent the clock feed-through.

Magnetic source

Requirements

The permanent magnet assembly must generate the magnetic field sensed by the detector. The field direction follows the rotation of the mechanism. This rotating element is composed of a mechanical structure that holds together the permanent magnet(s) in the desired configuration. Some of the main parameters of the magnetic source are listed thereafter.

- The magnetic field must lies within the chip plane. A small tilt is not an issue since a small and constant perpendicular component does not affects the angle reading.
- The magnetic field intensity must be large as an important field at the sensor position has two positive effects:
  - It increases the signal over noise ratio, which allows reducing the sensor bias current. This one limiting the power consumption and reducing the non linearity within the sensitive region that is the main cause of offsets.
  - It decreases the errors due to parasite external fields.
- The magnetic field must be homogeneous within the whole volume where the sensor is expected to move. This homogeneity is linked to the radius of homogeneity (HR) defined as the smallest distance from the center where the projection of the magnetic field in the sensor plan rotates by 0.05° (see Figure 8). HR varies with the distance along the z axis. The revolution of the function HR(z) around the z-axis defines the homogeneity volume.

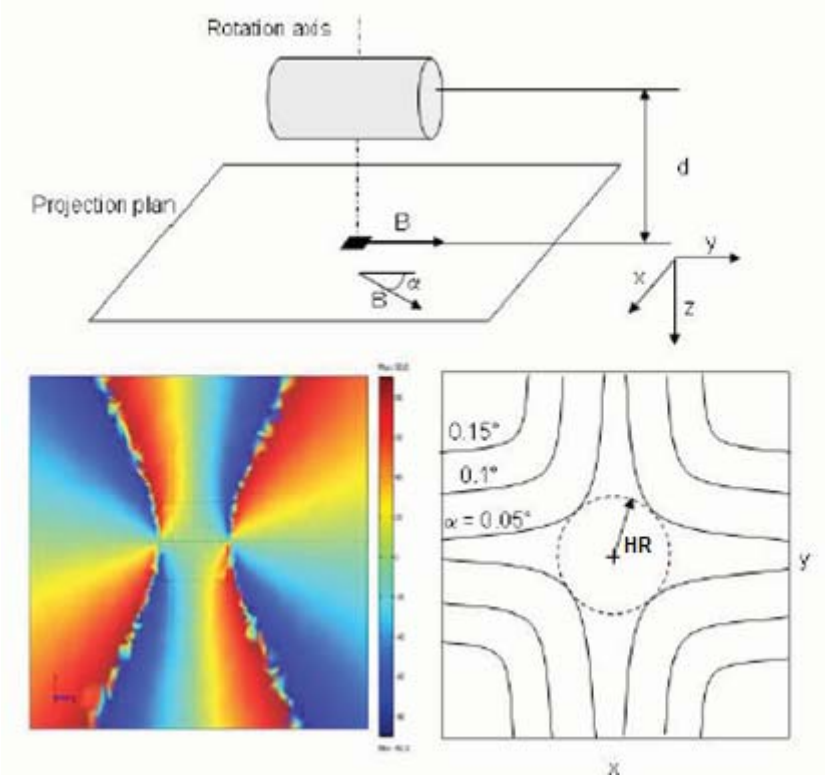

Figure 8. Definition of the homogeneity radius

- The stray field distance, depending on application, must be limited to reduce the field leaking out of the sensor region. A magnetic material (with high permeability) located inside the stray field region modifies the magnetic field distribution everywhere and thus might cause angular errors. In addition a small stray field offers a better compatibility with other nearby devices.
- The magnetic direction must be reproducible within the whole -60° to +90°C temperature range. Small changes in the field intensity does not directly affects the sensed angle, but in a real magnetic block, some region are usually close to demagnetization (corners, edges), and problem may arises when temperature induces a non uniform demagnetization. Therefore a magnet with

the smallest temperature coefficient is preferred. Similarly, radiations that can induce demagnetization must be limited.

Magnet material

The field intensity requirement imposes the use of rare earth magnets (meaning that one of the components is a lanthanide). The common compounds are NdFeB or SmCo. In general, NdFeB have a higher residual field (from 1 to 1.4 T instead of 0.8 to 1.1 T for SmCo) but this advantage is largely degraded by the other characteristics. First, SmCo has a smallest temperature coefficient (the reversible magnetism in SmCo decreases by 0.04 %/°C, which is about 10 times less than in NdFeB), higher Cure temperature and higher irreversible point (around 300°C for SmCo against 100°C for NdFeB), and therefore is less prone to irreversible loss of magnetism. As mentioned above, these effects are unwanted because a non-uniform demagnetization may lead to a change in the field orientation. Second, SmCo withstand radiation 2 to 40 times better than NdFeB. Finally, even though SmCo material is brittle and fragile, it is more resistant to corrosion and has a high resistance to oxidation. SmCo with the highest grade (corresponding to a higher coercively) are favorable to further improve the long-term stability. Among the highest grades, grade 28 is usually commercially available and is therefore a suitable material. The compound composition is Sm2Co17 and the blocks are fabricated by sintering. Its characteristics are listed in Table 1.

Table 1. Properties of SmCo28

Residual field (T)	Coercive field (kA/m)	Temp. coeff (%/°C)	Max working temp (°C)	Curie Temp. (°C)	Density (g/cm3)
1.03	760	0.04	300	800	8.3

Single magnet configuration

For production and magnetization simplicity the magnet assembly must consist of simple basic blocks (parallelepiped, cylinders, etc), with the magnetic moment orients and aligned with one edge.

For illustration, we show the performances obtained with a simple parallelepiped block (20 x 20 x 10 mm (x-y-z), magnetized along the x-axis). Figure 9 shows the field intensity and the HR as a function of the distance z from the magnet surface.

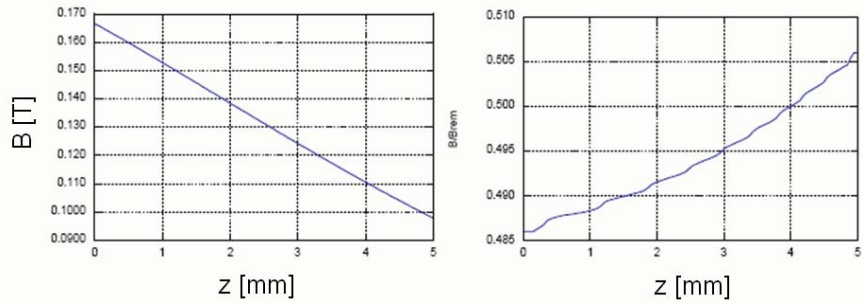

Figure 9. Field intensity (left) and homogeneity radius of a 20 x 20 x10 mm single block magnet

At 2 mm from the above single magnet surface (reasonable position of the sensor), the field intensity is around 140 mT and the homogeneity radius is 0.5 mm. These values comply with the homogeneity and intensity requirements. But the stray field distance is relatively large: 85 mm. Better performances in more compact configuration can be achieved with more complex magnet configurations.

Complex magnet configuration

The main idea is to constructively superpose the field from different magnet at the sensor location and destructively superpose at the outside. An arrangement known to allow this is the “Halbach” array [7]. Cylindrical Halbach array produce an intense field in a limited region and have a small stray distance because the total magnetic moment is zero. For the desired high accuracy, one suitable configuration consists in a Halbach crown made of 8 cubes, as shown in Figure 10. With fewer blocks, some volume is lost and with more blocks, the elementary cube is too small and the field intensity decreases (it is roughly proportional to the cube volume) [RD5]. A stack of two such crowns improves the field homogeneity and gives some displacement freedom along the z-axis (rotation axis). A comparison between the field

intensity and the homogeneity radius of a double-crown and a single-crown configuration is presented in Figure 11.

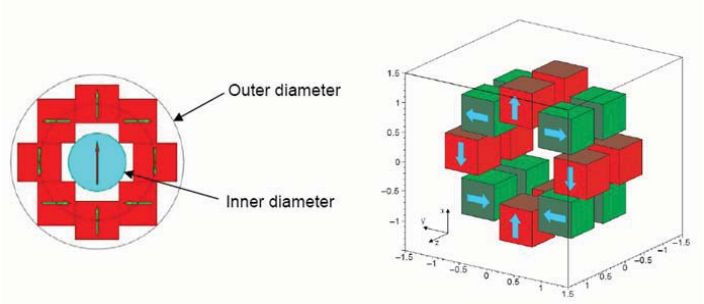

Figure 10. Left: Halbach crown made of 8 cubes in close contact. Right: Double crown configuration.

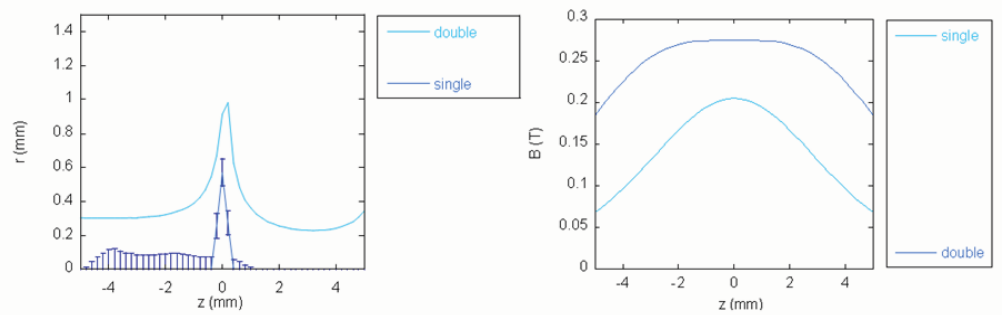

Figure 11. Comparison between a double and a single crown magnets configuration in terms of homogeneity radius and field intensity.

Table 2. Magnet assembly (dimensions in mm).

Outer diameter	Inner diameter	Height (along z)	Cube side	Cube pitch	Cube center radius
19	7.7	9.7	4	0.7	6.7

The angular homogeneity produced by the assembly with the parameters defined in Table 2 in the centre plane (z = 0) is shown in Figure 12. The homogeneity radius is close to 1 mm. Effect of displacements, errors in cube positioning, sizes and imperfection in the magnetization show that a displacement of the order of 0.1 mm affects the homogeneity radius by an amount of the same magnitude. The field intensity produced by the magnet assembly is around 270 mT. This relatively high value allows limiting the sensor bias current and thus decreasing the offsets. The stray field distance is 22 mm, i.e. about 10 mm out of the external diameter. The value is well below the values obtained for non-zero magnetic moment assemblies (like a single block solution).

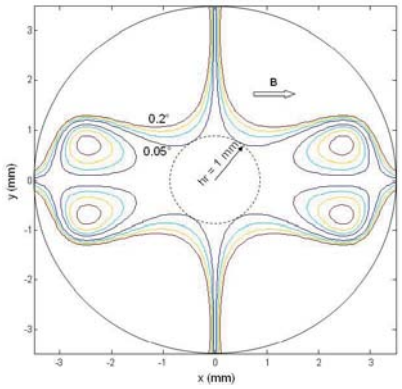

Figure 12. Angular homogeneity in the magnet center plane (z = 0) for a double-crown configuration.

Technology qualification campaign

Setup

The whole APS sensor is tested during the technology qualification campaign. The final test configuration dedicated to the tests is illustrated on Figure 13. The rotating element is mounted on a shaft guided trough a bearing system and drive by a precision actuator. An optical encoder, offering a high accuracy, is mounted on the actuator and represents the reference sensor. A decoupling between the APS and the driving system allow keeping the same configuration in a thermal vacuum (TV) chamber where a vacuum feedtrough is inserted between both systems.

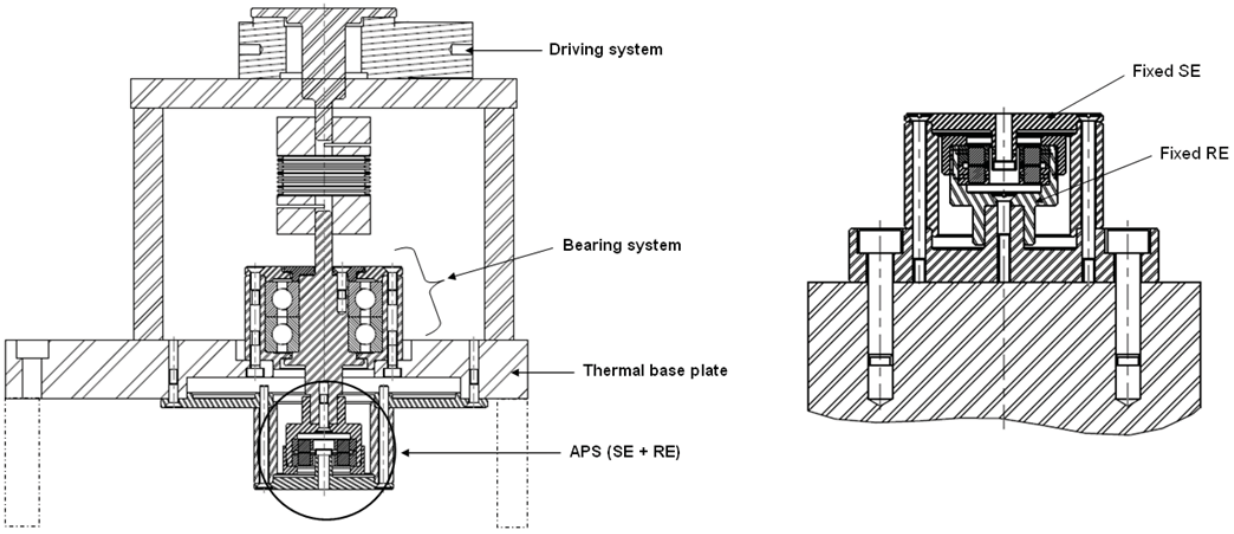

Figure 13. Left: APS functional and TV test setup. Right: APS setup for vibration, shock and radiation tests.

The technology qualification tests start at the reception of the Multiple Process Wafer run (MPW) with the plan detail thereafter. Standards procedure related to the test are also listed.

Packaging of the chip and package tests

- Visual inspection [ECSS 20500]
- Bond strength [MIL-STD-883]
- Die shear [MIL-STD-883]
- Encapsulation
- Dimension check: The outline dimension and envelope of both rotating element and sensing element are inspected according to the interface drawing.
- Weight: The weight of the unit, including the flying leads shall be less than 100g according to the sensor specifications.

Performance functional tests

- Range: The unit should be able to rotate without any limitation. 2 complete rotations are performed in both directions.
- Absolute measurement: The objective of this test is to verify that the sensor is not only an incremental sensor and that the angular position of the magnetic field can be recovered even after a shut-down of the power-supply.
- Accuracy: Following the sensor specification, the accuracy of the APS should be closed to 0.05°. The noise level gives a good representation of the minimum accuracy that can be reached by the sensor. However, this noise level depends on the electronic placed back along the sensor, in particular the RC filter used to convert the PWM output into an analog signal. The bit accuracy of the digital signal is most appropriate illustrate the real accuracy of the sensor. The noise of the analog output is also monitored for comparison. An angular accuracy of 0.05° corresponds to an analog voltage noise of Vcc/7200, i.e. less than 460 μV. This corresponds to a digital output on 13 bits, i.e. three bits of noise on the 16 bits channel.

- Resolution: The minimum incremental motion of the driving stage used to rotate the functional setup is defined to 0.004°. With such a resolution, the resolution of the APS can be investigated.
- Repeatability
- Drift parameters: Leakage current at several level of the chip layout, bandgap voltage are some of the drift parameters which can be influenced by radiation, EMC and temperature range and which are monitored.

The objective of the functional tests is to verify the specifications under environmental constrains describes in the next sections. These functional tests are repeated at reception of the chip, after the radiation test, after the vibration and shock campaign, after the EMC test and after the lifetime test.

Radiation test

The test is performed at the Proton Irradiation Facility of the Paul Scherrer Institute (PSI) in Villigen (Switzerland). Total Dose Irradiation (TID according to ESCC 22900) test and Single Event Effect (SEE according to ESCC 25100) test is performed. During the test, the sensing element is protected by a minimum of 4 mm Aluminum inner wall (sketch on Figure 13) that allows estimating the total dose for a worst-case 15-year radiation lifetime of a geo-stationary telecom satellite. The parameters of the radiation tests are the following:

- Proton Energies6 MeV
- Total dose: 300 krads
- Maximum flux: 100 rad/h

During the irradiation, the sensing element is facing a static permanent magnet, which allows for the monitoring of drift parameters of the sensor such as the leakage current that is monitored at several level of the block diagram or several parity bits that allow for the SEE detection. The output of this radiation test validates the hardening of the design that is implemented in the second chip layout.

Vibration and shock tests

The test sequence comports Sine vibration test, random vibration test and shock test. These tests are performed on the three axes of the sensor. The vibration tests are made at room temperature, in air and the unit is neither powered nor rotating. The APS setup (including the dummy shaft) is mounted on a dedicated test support fixed on the shaker for the vibration tests (Figure 13). The setup is first tested without the APS in order to identify frequencies related to the tooling itself. Vibration and shock loads are summarized in Table 3:

Table 3. Vibration and shock loads

Vibration	Test Axis	Input Frequency (Hz)	Amplitude	Duration
A) Sine Vibration	All 3 axis	20 – 50	25 mm peak (or max shaker limit)	2 oct/min +/- 10% (minimum duration 2 min)
		50 – 100	20 g	2 oct/min +/- 10% (minimum duration 2 min)
Sine vibration sweep rate:		2 octaves/minute (+/- 10%)		
Sine vibration duration:		2 minutes/axis (minimum) (+/- 10%)		
B) Random Vibration	All 3 axis	20 –100	+5 dB/oct	150 seconds
		100 – 500	0.5 g^2/Hz	150 seconds
		500 - 2000	-5 dB/oct	150 seconds
		Overall level :	20 g_{rms}	
Random vibration duration:		2.5 minutes/axis (+/- 10%)		
C) Shock	All 3 axis	500	100 g	-
		5000	1500 g	-
		10000	1500 g	-

Thermal vacuum test

The APS is installed in a thermal vacuum chamber with its rotation axis vertically mounted. The sensing element and its packaging is fixed on a thermal base plate inside the chamber in order to control the temperature of the APS mounting flange by conduction. The anodized support acts as a frame surrounding the APS in order to promote radiative exchanges. The APS is thermally cycled in vacuum (< 10^{-5} Pa) according to Figure 14.

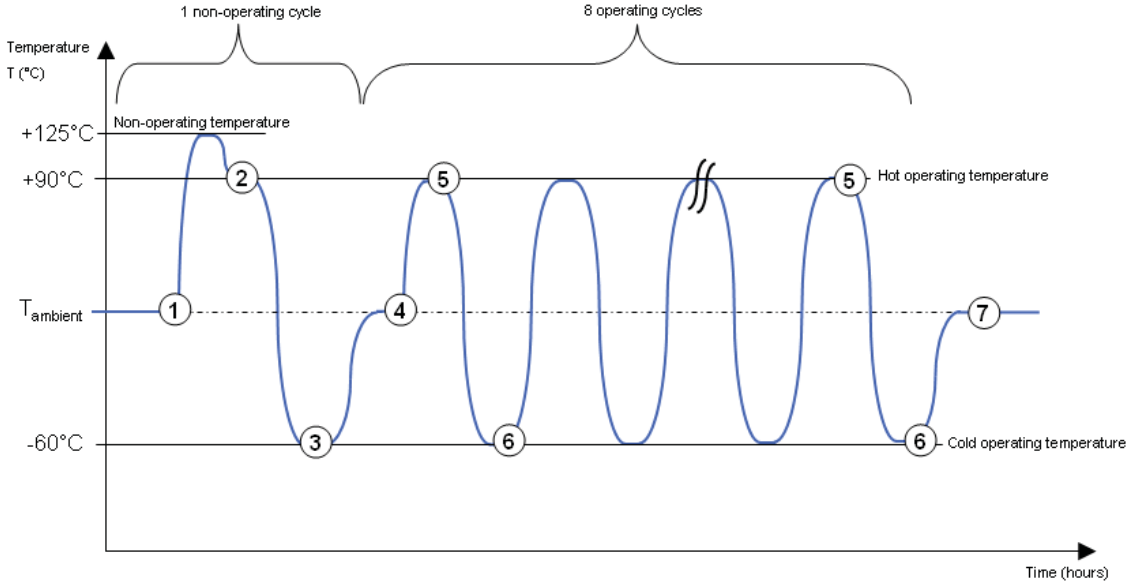

Figure 14. Thermal cycles performed on the APS.

The following operations occur during the thermal vacuum test:

- ① Thermal balance and non-operating cycle.
- ② Hot non-operational performance functional test.
- ③ Cold non-operational performance functional test.
- ④ Performance functional test at ambient temperature. Power switch on.
- ⑤ Hot operational performance functional tests (at 1 and 8th operating cycle)
- ⑥ Cold operational performance functional tests (at 1 and 8th operating cycle)
- ⑦ Performance functional test at ambient temperature. Power and rotation switched off.

The following parameters are monitored continuously during the operating cycles of the APS:

- Temperature of the various thermal probes
- Digital Output
- Analog Output
- Bandgap Voltage
- Driving torque (drag torque of the APS)
- Pressure

EMC test

Electromagnetic compatibility is the ability of electrical equipment to work satisfactorily in its electromagnetic environment without affecting this environment in an inadmissible way. The electromagnetic compatibility of the APS is verified by means of tests performed at frequency range between 10 kHz and 18 GHz in an anechoic room. The tests consist in the measurement of the radiated and the conducted disturbance immunity of the sensor (susceptibility) and to its emissivity in accordance with standard ECSS-E-10-03A.

Lifetime test

The APS sensor is thermally cycled in vacuum (< 10^{-5} mbar) between cold and hot operating temperatures (-60°C/+90°C). As the sensor includes micro-electronic parts, the number of thermal cycles (100) is adapted to such electronics systems.

Chip qualification campaign

In parallel of the previous TRP activity, a complete qualification of the chip itself, in accordance with space standards for the qualification of monolithic chip, is undertaken. Tests foreseen in this chip qualification activity can be divided in three steps:

- The production control tests which occur at the manufacturer level
- The screening tests
- The qualification tests

Production control tests

The wafer lot acceptance tests occur at the manufacturer level: The manufacturing of the wafers is monitor and PVM data are recorded during the whole process. The final lot is inspected through scanning electron microscope.

Then, in-process controls occur at the packaging level: After a pre-encapsulation visual inspection, bond strength and die shear tests are implemented. After the chip encapsulation, a dimension check of each packaged chip is performed.

Screening tests

These tests are performed on all the components. Screening tests consist mainly to reject faulty chips though hard electrical and temperature testing. During those tests, the drift parameters of the chip are monitored and compare to failure criteria. The following tests are foreseen:

- The serialized chips are subjected to a high temperature stabilisation bake (24h at 150°C) to determine the effect of storage at elevated temperatures without electrical stress applied. Drift parameters are monitored and control during the entire test.
- The chips are then be subjected to several burn-in tests at 125°C (reverse bias and power burn-in) in order to eliminating marginal devices, those with inherent defects which cause time and stress dependent failures. Drift parameters are monitored and control during the entire test.
- A measure of the drift parameters at ambient temperature is then foreseen and allow for the lot qualification.
- Before a final visual inspection of each chip, test of the quality of the package sealing are foreseen as well as evaluation of the ability of the terminations of the package for solderability.

Qualification tests

The parameters of these tests are the same as presented in the technology qualification campaign. These tests are performed on a minimum of 45 chips. 3 subgroups are constituted and follow respectively:

- Mechanical tests (15 chips): Vibration, shock, constant acceleration and seal tests followed by a visual inspection are foreseen in this subgroup. Drift parameters are measured along the tests.
- Environmental tests (15 chips): Thermal shock, moisture resistance and seal tests followed by a visual inspection are foreseen in this subgroup. Drift parameters are measured along the tests.
- Endurance tests (15 chips): Lifetime and seal tests followed by a visual inspection are foreseen in this subgroup. Drift parameters are measured along the tests.

Conclusion

The absolute angular position sensor presented here offers several advantages over common conventional potentiometer for space applications; based on a contactless technology, it offers a high reliability for long-term lifetime missions. Combining a Hall ring sensitive structure and control electronics with modern CMOS technologies, it gives the possibility to manufacture miniature accurate sensors. With this technique, the angular position can be obtained by a simple phase detection method, increasing the reliability of the whole system for harsh space environments.

The device has already been tested in ambient condition [8] and the results fulfill the expected performance of the sensor gathered in Table 4. The technology qualification of the sensor has just started and will be followed by the qualification of the chip itself. The reliability against vibration and shock loads is not considered as an issue for a sensor with such dimensions. Thanks to both radiation tests, one within the TRP activity before the other during the chip qualification campaign. The reliability of the chip against radiations (TID and SEE), allows for a progression margin and to a complete validation of the layout radiation hardness. Last point, but not least, is to verify the stability of the high accuracy of the sensor along the whole temperature range (define actually to -60°C to +90°C) and, with regards to the results, to propose an upgraded range of functional temperatures to increase the space applications panel covered by this contactless angular position sensor.

Table 4. Functional performances of the APS sensor

Specifications	Value
Operational lifetime	> 10.10^6 (theoretically ∞)
Orbit lifetime	> 15 years
Storage lifetime	5 years
Weight	< 100g (magnetic configuration depending)
Mechanical range	360° continuous
Measurement type	Absolute
Speed of rotation	< 1 RPM
Accuracy	≤ 0.05°
Resolution	< 0.01 °
Repeatability	< 0.01 °
Stability	< 1 ppm/°C

References

1. "Angular Position Sensor based on MEMS Technology", ESTEC/Contract No. 20404/06/NL/CP.
2. http://lmis3.epfl.ch/
3. Law L. "Angular Position Sensing with 2-axis Hall ICs", *Sensors* (http://www.sensorsmag.com), March 2003.
4. Volder J. E. "The CORDIC Trigonometric Computing Technique", IRE transactions on ElectronicComputers, vol. EC-8, no. 3, 1959, 330-334.
5. Popovic R. S. "Hall Sensor and Method of Operating a Hall Sensor", Patent number EP1679524 A1, 12.07.2006.
6. Popovic R. S. "*Hall Effect Devices*", Adam Hilger (IOP – Institute of Physics Publishing), 2nd edition, 2004, pp. 261-264.
7. Raich H. "*Design and Construction of a Dipolar Halbach Array with a Homogeneous Field from Identical Bar Magnets: NMR Mandhalas*", Concepts in Magnetic Resonance Part B (Magnetic Resonance Engineering), Vol. 23B, 2004, pp. 16-25.
8. Reymond S., "True 2D CMOS integrated Hall sensor", IEEE sensors 2007.